



OPEN ACCESS

EDITED BY

Huan-Cheng Chang,
Academia Sinica, Taiwan

REVIEWED BY

Romana Schirhagl,
University Medical Center Groningen,
Netherlands

*CORRESPONDENCE

Philip R. Hemmer,
✉ prhemmer@exchange.tamu.edu
Masfer H. Alkahtani,
✉ mqhtani@kacst.edu.sa

RECEIVED 07 April 2023

ACCEPTED 11 May 2023

PUBLISHED 02 June 2023

CITATION

Alkahtani MH, Alzahrani YA and
Hemmer PR (2023), Engineering sub-
10 nm fluorescent nanodiamonds for
quantum enhanced biosensing.
Front. Quantum Sci. Technol. 2:1202231.
doi: 10.3389/frqst.2023.1202231

COPYRIGHT

© 2023 Alkahtani, Alzahrani and Hemmer.
This is an open-access article distributed
under the terms of the [Creative
Commons Attribution License \(CC BY\)](#).
The use, distribution or reproduction in
other forums is permitted, provided the
original author(s) and the copyright
owner(s) are credited and that the original
publication in this journal is cited, in
accordance with accepted academic
practice. No use, distribution or
reproduction is permitted which does not
comply with these terms.

Engineering sub-10 nm fluorescent nanodiamonds for quantum enhanced biosensing

Masfer H. Alkahtani^{1,2*}, Yahya A. Alzahrani² and
Philip R. Hemmer^{1,3*}

¹Institute for Quantum Science and Engineering, Texas A&M University, College Station, TX, United States

²Future Energy Technologies Institute, King Abdulaziz City for Science and Technology (KACST), Riyadh, Saudi Arabia, ³Department of Electrical and Computer Engineering, Texas A&M University, College Station, TX, United States

There is an increasing interest in the sensing of magnetic, electric, and temperature effects in biological systems on the nanoscale. While there are existing classical sensors, the possibility of using quantum systems promises improved sensitivity and faster acquisition time. So far, much progress has been made in diamond color centers like the nitrogen-vacancy (NV) which not only satisfy key requirements for biosensing, like extraordinary photostability and non-toxicity, but they also show promise as room-temperature quantum computers/sensors. Unfortunately, the most-impressive demonstrations have been done in bulk diamond, since NVs in fluorescent nanodiamonds (FNDs) tend to have inferior properties. Yet FNDs are required for widespread nanoscale biosensing. In order for FND-based quantum sensors to approach the performance of bulk diamond, novel approaches are needed for their fabrication. To address this need we discuss opportunities for engineering the growth of FNDs.

KEYWORDS

nanodiamonds, low pressure and low temperature, hydrothermal growth, nitrogen-vacancy center, quantum sensing

1 Introduction

Diamonds have attracted special attention in many promising application areas due to their optical properties (tunable absorption and emission based on a wide variety of color centers), surface chemistry, and biocompatibility (Alkahtani et al., 2018). These applications include quantum information (Maurer et al., 2012; Pezzagna and Meijer, 2021), advanced bio-sensing including drug delivery (Alkahtani et al., 2018; Miller et al., 2020), hyperpolarized magnetic resonance imaging (MRI) (Waddington et al., 2019), nanoscale imaging down to the single protein level (Hemmer and Gomes, 2015), and advanced materials diagnostics, especially for magnetic materials and superconductors (Dovzhenko et al., 2016). In particular, small sized (less than 10 nm) and round shaped FNDs with properties comparable to bulk diamonds are critical for many biological applications. Such small and high-performance FNDs have the potential to pass through the nuclear membrane, and have theragnostic applications like drug delivery (Perevedentseva et al., 2021; Chang et al., 2022) because they can be quickly cleared through kidney cells (Chang et al., 2022).

Commercially available small FNDs (with size less than 10 nm) are fabricated either by top-down approaches like crushing bulk diamonds that were previously grown at high pressure and high temperature (HPHT) (Boudou et al., 2013), or bottom-up production of

nanodiamonds by detonation (DNDs) (Qureshi et al., 2022) or related techniques. Unfortunately neither approach gives nanodiamonds of sufficient quality to achieve bulk-like sensing performance, especially for the NV (Chang et al., 2022). This is attributed to crystal and/or surface defects that can act as spin and charge traps. In addition, the random distribution of color centers in very small NDs crystals results in additional inhomogeneities due to different distances of each color center from the surface. This is important because surface interactions can quench fluorescence, for example, via energy or charge transfer, and/or reduce spin coherence times, both of which significantly reduce the sensitivity for quantum sensing applications (Chang et al., 2022). Even ensuring that there is at least one-color center in small nanodiamond is a challenge. For these reasons, small diamond nanocrystals have so far only been used in proof-of-concept experiments, for example, with NV (Kaviani et al., 2014; Karim et al., 2020) and silicon-vacancy (SiV) (Vlasov et al., 2014) color centers. Significantly the SiV work showed the tantalizing possibility of using NDs with sizes comparable to those of biological fluorescent molecules like green fluorescent protein (GFP) (Funatsu et al., 2002). Unfortunately, there are still no reliable or scalable fabrication methods to produce these, though some recent growth demonstrations are closing the gap (Davydov et al., 2014; Liu et al., 2022).

One way to overcome the above-mentioned limitations, would be bottom-up synthesis of NDs from molecular precursors which can lead to small FNDs with optically color centers precisely located in the nanocrystals. This idea originated decades ago with some encouraging recent results (Dahl et al., 2010; Tzeng et al., 2017; Alkahtani et al., 2019). The basic idea is simple; since it is hard to control both growth and nucleation of nanodiamonds at the same time, diamond-like molecules could serve as nucleation seeds, and the growth could be then optimized for high-quality diamond without the conflicting requirements for spontaneous nucleation. However, thus far the problem with this approach has been poor yield, defined as percentage of seed molecules converted to nanodiamond. Apparently diamondoids do not seed the growth of nanodiamonds with high yield unless they are larger than some unknown threshold that is beyond existing efficient chemical synthesis methods.

To address these scalability problems, we assert that existing nanodiamond growth techniques are overly complicated. Contrary to popular belief, there is no clear reason why highly-controlled, equilibrium growth of small nanodiamonds should not be practical even at atmospheric pressure. If true this would eliminate the need for expensive high-pressure apparatus, nonequilibrium detonation techniques, and even rate-equation based chemical vapor deposition (CVD) techniques. In fact, thermodynamically speaking, it should be easier to produce nanodiamonds (below 10 nm) than to produce other carbon forms like bucky-onions, carbon nanotubes, or even graphene. Convincing experimental and theoretical evidence for this was published long ago (PENG et al., 2001). Apparently, one need only ensure that the surface remains hydrogen-terminated throughout the growth process. Provided this is done, one should be able to use any thermal, catalytic, electrochemical, or other means to enhance growth rate and/or increase the yield of molecule seeded, or even self-seeded growth.

Spurred by this knowledge, a handful of researchers have explored a number of theoretical and experimental techniques for

nanodiamond growth from a variety of precursors and under a variety of experimental conditions, even some at low-pressure and low-temperature (LPLT). For instance, it was theoretically predicted that sub-7 nm small nanodiamonds can be grown from hydrocarbons and graphene precursors at LPLT (Badziag et al., 1990; Stein, 1990). This prediction has been experimentally realized by synthesis of small NDs in many experiments (Lewis et al., 1987; PENG et al., 2001; Dahl et al., 2003; Su et al., 2011b; Kumar et al., 2013a). Recently, it has even been claimed that hydrothermal techniques can grow sub-4 nm NDs from nitrated hydrocarbons and graphene at a very low temperature of (423 K) (Shen et al., 2021). The latter are exciting because, if successful, they would allow any researcher with a pressure cooker to produce their own high-quality nanodiamonds.

A recent summary of non-conventional nanodiamond growth approaches is comprehensively covered in (Chang et al., 2022). However, it should be noted that most of these papers do not provide convincing evidence that they actually succeeded in growing nanodiamonds. For example, often there is only one diagnostic showing evidence of diamond production, for example, Raman spectra or transmission electron microscope (TEM) images, but not both. Since there are a number of materials having a similar Raman spectrum to diamond, and others having similar lattice spacings, we have concluded that a key property that is needed to rule out false positives is the observation of a fluorescent color center unique to diamond, like a magnetically sensitive NV or a SiV with its well-known optical spectrum. Indeed this was the technique used to identify the world's smallest high-quality nanodiamonds in meteors (Vlasov et al., 2014).

In this perspective, we will discuss some of the most promising approaches to direct growth of high-quality, small NDs (with size less than 10 nm). A key part of this discussion will be preliminary results from our own attempts to reproduce and extend some of these techniques, where we emphasize the creation of diamond color centers to prove that diamond was actually grown. We also show that the properties of these color centers can be used to provide a measure of the quality of nanodiamonds, in particular their suitability for emerging quantum imaging and sensing applications. Here it should be noted that the color center properties can also be used to determine whether the diamonds were actually produced by the growth technique or were introduced as a contamination. In what follows we will mostly discuss liquid-based growth, rather than "low temperature" CVD techniques that require vacuum, plasma, and/or cracked atomic gases. Many of these vacuum techniques show convincing evidence of nanodiamond growth, but require more expensive and sensitive equipment. They are also more difficult to scale up to kilogram quantities of dispersed nanodiamonds, because the growth is inherently surface-based, so that the product must somehow be continually removed from the surface to produce large quantities of nanodiamonds.

2 Growth of fluorescent nanodiamonds at high pressure and moderate temperature

It was shown that high-order diamondoid molecules and even nanodiamonds can be found in petroleum (Dahl et al., 2003).

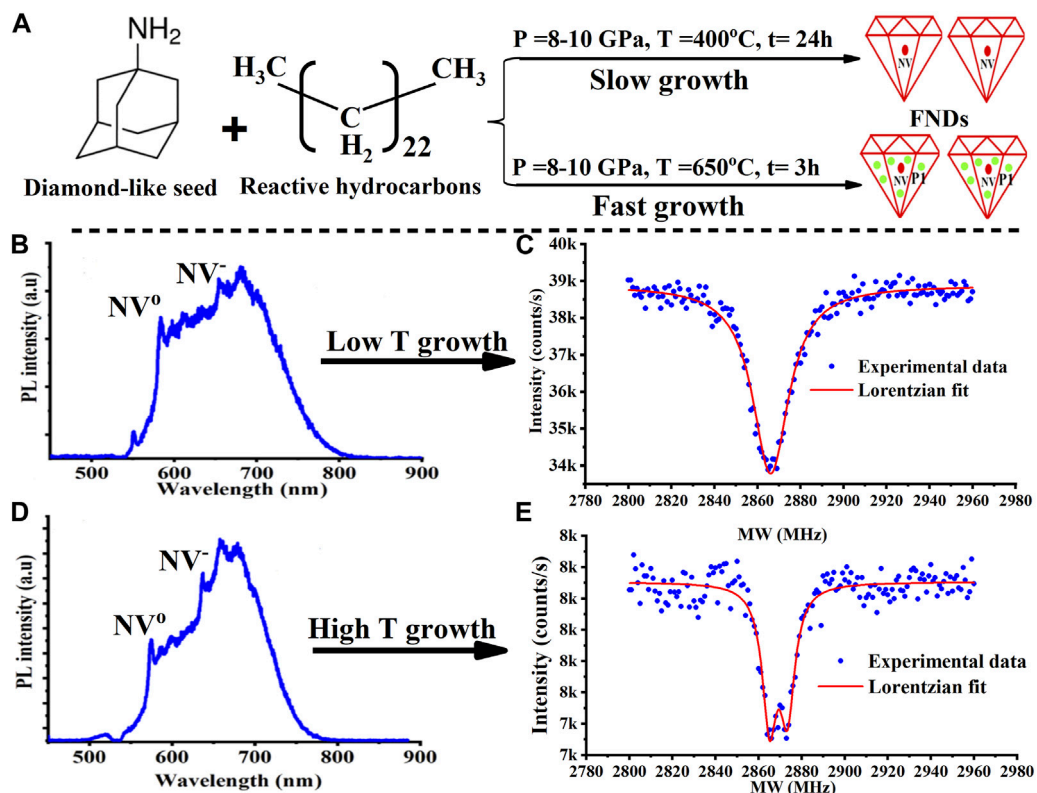


FIGURE 1

Impurity incorporation into diamond as a function of growth temperature. (A) An illustration explains how nitrogen impurity concentration is expected to depend on growth temperature. The growth mix consisting of 1-Adamantylamine, heptamethylnonane, tetracosane, and tetramethylhydrazine was exposed to a high pressure (10 GPa) and then either low or high temperature in diamond anvil cell (DAC) for 24 h. (B) At low growth temperature (400°C), nitrogen irradiation and annealing is needed to see the NV center optical emission. In this case there are also too few nitrogen P1 centers to keep the NV charge stable upon blue illumination as evidenced by the higher fraction of NV⁰. (C) Additional evidence that little nitrogen grows into the diamond is the lack of zero-field splitting in the optically detected magnetic resonance (ODMR) line. In contrast, as shown in (D), the NV spectrum from nanodiamonds grown at high temperature is stable under blue illumination. (E) Additional evidence of a larger nitrogen concentration is the zero-field splitting on the ODMR. At this growth temperature the NVs were sometimes seen even without nitrogen irradiation or annealing.

Spurred by this, several researchers have attempted to reproduce these results. The most successful were done using CVD techniques in which diamondoids were anchored to the growth wafer (Tzeng et al., 2017). Recent work by these groups shows that the diamond yield (fraction of nanodiamonds produced per diamondoid molecule) was a strong function of the order, or size, of the diamondoid molecule (Park et al., 2020). However in the liquid phase the emphasis was mostly on the creation of larger diamondoids (Dahl et al., 2003).

Since petroleum-based diamondoid growth is assumed to proceed at high pressure, we first attempted to reproduce and extend these results using a diamond anvil cell (DAC) (Alkahtani et al., 2019; Alkahtani and Hemmer, 2020). In contrast to most prior experiments, we emphasized the use of a nitrogen-containing diamondoid seed molecule with the aim of eventually producing nanodiamonds with a deterministic number of NVs. In a typical experiment, a diamond-like organic molecule (2-azaadamantane hydrochloride or 1-adamantylamine) was mixed with reactive sp³-rich hydrocarbons such as tetracosane and heptamethylnonane as illustrated in (Figure 1A) (Zapata et al., 2017; Alkahtani et al., 2019). Growth was carried out at a

relatively low temperature; chosen to be below the decomposition temperature of the diamondoid seed molecule but near the temperature where the other hydrocarbons crack. In this way, the hydrocarbons were assumed to provide a source of reactive carbon, like methyl radicals, needed for diamond growth. In one example a 10 GPa pressure and 400 C temperature was applied for 24 h. In this case, the grown FNDs show a clear NV center spectrum as demonstrated in (Figure 1B). Here it should be noted that nitrogen implantation followed by high temperature vacuum annealing was required to produce NV centers in this case.

As mentioned above, this NV can be used as a diagnostic of diamond quality. To illustrate this, we note that the optical spectrum in (Figure 1B) was excited with a blue laser. With green laser excitation (not shown) there is a much larger fraction of NV⁻ (almost 2 X). This suggests a low nitrogen content, especially of nitrogen-donor P1 centers, in the neighborhood of the NV. This interpretation is also supported by the optically detected magnetic resonance (ODMR) spectrum in (Figure 1C), which shows a high-contrast of 12.8% and a narrow line width with mean \pm standard deviation (SD) equal to 17.35 ± 3.07 for 13 samples. To understand why the nitrogen content is low, we note that when crystals are

grown slowly, they tend to exclude impurities. In the present case, growth temperature controls growth speed through the hydrocarbon cracking rate which in turn controls the concentration of reactive carbon (like methyl radicals). Therefore, the lower the growth temperature, the slower the growth rate. In addition, self-nucleation is expected to be suppressed by the low concentration of reactive carbon, so that the presence of a diamodoid seed molecule, or other nucleation agent, should become more important. Indeed, we do not see diamonds without these seed molecules in the growth mix.

To test the above slow-growth hypotheses, we repeated the growth at a higher temperature ($\sim 650^{\circ}\text{C}$) as shown in (Figures 1D, E). At this temperature, in addition to faster growth, even the diamodoid molecule is expected to decompose so that self-seeding is expected to occur. As seen, the NV centers in nanodiamonds grown at this temperature have better NV- charge stability when excited by a blue laser (Figure 1D). In fact, the emission spectra for both blue and green excitation become identical. This suggests there are more nitrogen-donor P1 centers near the NV. In agreement with this, a slightly larger zero-field ODMR splitting is also seen (Figures 1C vs 1E). The ODMR line width of NV centers grown at high temperature was measured to be equal to 23.44 ± 3.04 for 9 samples. Although the differences between the two ODMR lines aren't large enough to be statistically significant for our small sample size, it is clear that the zero-field splitting is still much less than for NVs in commercial crystals with a high nitrogen concentration. In agreement with this, our past laser-heating experiments, with growth temperatures in excess of $1,500^{\circ}\text{C}$, produced NVs with well-resolved zero-field splitting (not shown).

3 Growth of fluorescent nanodiamonds at atmospheric pressure

As mentioned above, other attempts were made to grow diamonds at low pressure, for example, using organic hydrocarbons in inert atmosphere at a temperature of $\sim 1,000^{\circ}\text{C}$ (Visscher et al., 1993). Still more experiments along with theory explained how nanodiamonds could form at atmospheric pressure under a variety of conditions including meteors (Lewis et al., 1987), molten lithium chloride (Kamali and Fray, 2015), petroleum (Dahl et al., 2003), detonation soot (Greiner et al., 1988), candle flames (Su et al., 2011a), and micro-plasma (Kumar et al., 2013a).

To evaluate these claims, we decided to try to reproduce some of these low-pressure diamond growth experiments. As for high pressure growth, we emphasized the use of nitrogen-containing seed molecules, with the eye toward eventually producing a deterministic number of color centers. Again, this necessitated the use of low growth temperatures where the seed molecule is stable but there is controlled decomposition of some other molecule that produces reactive carbon.

Our first low-pressure growth attempt approximately followed the high-pressure growth chemistry described above. However, we also included a versatile solvent, dimethyl sulfoxide (DMSO), to improve the solubility of the amine-containing seed molecule with our non-polar hydrocarbon growth material. DMSO has the additional advantage that it produces methyl radicals at an even lower temperature than our organic hydrocarbons. But it has the disadvantage of having oxygen atoms. Typically, growth was done for

about 24 h, either in a reflux column at atmospheric pressure or in a autoclave at a slightly higher temperature near 220°C for 24 h.

After growth, the sample was typically purified by oxidizing in air for ~ 10 min at 550°C to remove excess organic growth material, graphite and most of the diamond-like carbon (where applicable). To create color centers, these samples (small NDs with size 5–7 nm) were then irradiated with silicon atoms at a low energy of 3 KeV and annealed at $1,100^{\circ}\text{C}$ for 1 hour in vacuum. As seen in (Figure 2), diamond SiV color centers were produced, proving that diamond was indeed grown.

In spite of the expected low nitrogen concentration, we observe a stable NV⁻ charge under green excitation, as illustrated by the suppressed NV⁰ emission in (Figure 2B). While we do not know the reason for this charge stability we note that recent work on sulfur implantation shows that sulfur-rich diamond produces NVs with stable negative charge (Lühmann et al., 2021). Since DMSO is very sulfur-rich, some incorporation of sulfur into our nanodiamonds is reasonable.

While we have not yet measured the NV yield vs. implanted silicon ion, we note that for shallow implantation, the NV yield is usually less than a few percent, whereas it is typically much higher for silicon-vacancy (SiV) (Flatae et al., 2020). The fact that every SiV is co-located with a NV (Figures 2B, D) suggests either high P1 concentration or high NV yield. The narrow ODMR spectrum of [Figure 2B(inset)] points to low P1 concentration. At the same time sulfur doping would be expected to increase NV yield upon irradiation (Lühmann et al., 2021). (Alkahtani et al., 2023).

4 Growth of small nanodiamonds at LPLT from nitrated aromatic hydrocarbons

As mentioned earlier, it was recently reported that sub-4 nm NDs can be grown at a low-temperature (423 K) via a hydrothermal approach by using graphene-oxide or nitrated polycyclic aromatic hydrocarbons such as naphthalene, anthracene, phenanthrene, or pyrene (Shen et al., 2021).

To investigate this approach, we decided to reproduce this result, again concentrating on the creation of diamond color centers to supplement the other diagnostics. Our experiments showed that a higher growth temperature near 493 K for 24 h was required to form diamond as illustrated in (Figure 2E). After the reaction was complete, a thorough cleaning was performed using dialysis for several days to remove residual growth chemicals and residues without losing any small NDs.

Raman spectroscopic analysis with green excitation (532 nm laser), showed a strong and broad diamond Raman line at $1,328/\text{cm}$, partly overlapping weak D and G peaks characteristic of amorphous carbon, (see Figure 2F). After further optimization of the growth chemistry, the TEM images show an increasing yield of small and dispersed nanodiamond with size 5–7 nm, as illustrated in (Figure 2G). The diffraction pattern of cubic diamond with the correct (111) lattice spacing was confirmed for these nanodiamonds as shown in (Figure 2G) (Kumar et al., 2013b).

To create diamond color centers, we plan to implant these nanodiamonds with silicon as before. However, until this can be done, we went ahead and performed the vacuum anneal that is normally done after implantation (i.e., 700°C for 10 min). This was

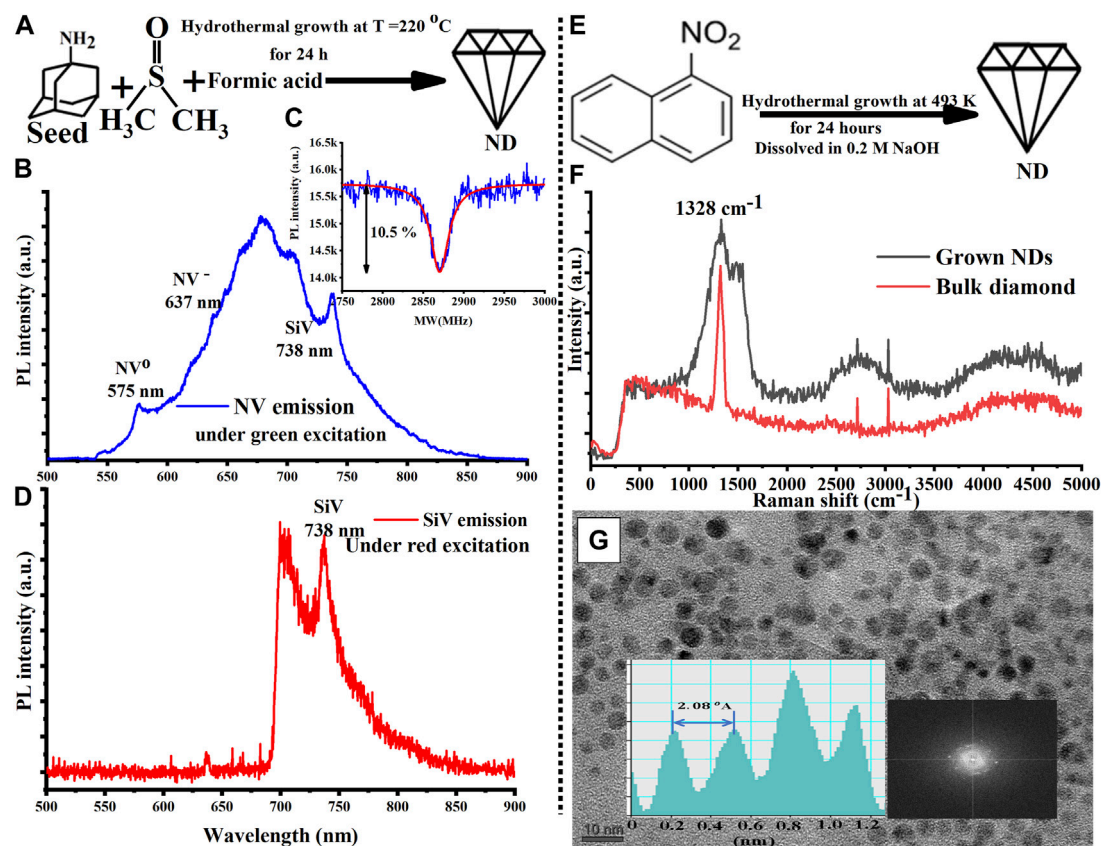


FIGURE 2

(A) An illustration of the concept of nanodiamond growth near atmospheric pressure. Basically, diamond-like template molecules, DMSO, and formic acid were mixed placed in a hydrothermal growth vessel at 220°C for 24 h. In the NV center optical emission in (B), the NV⁰ fraction is small, indicating stable NV- charge. (C) The ODMR doesn't show a significant zero field splitting suggesting low nitrogen content. It has a high contrast near 11%. (D) The silicon-vacancy becomes more visible when exciting with 660 nm laser light. (E) A schematic illustration of small NDs with size (5–7 nm) grown from aromatic hydrocarbons at mild hydrothermal conditions. Experimentally, a nitrated naphthalene precursor was mixed with 0.2 M of NaOH and then transferred into a hydrothermal vessel and heated to 220°C in a oven for 24 h to grow the diamond. (F) Raman spectrum of the synthesized NDs compared to a Raman spectrum of known diamond bulk crystal. (G) High magnification TEM image of the synthesized NDs where an FFT showed a cubic-diamond diffraction pattern with the correct (111) lattice spacing. A few NVs were created in this sample through vacuum annealing, even though we didn't have access to an ion implanter.

done, because our past experiments have shown that even without irradiation, NV centers are sometimes produced with low yield, even without irradiation. As shown, NV centers were indeed formed, and their properties were very different from the commercial nanodiamonds we normally use in the laboratory. Measurements of T1 for these particles is still in progress but will take time because of the need to correlate crystal size with T1. Nonetheless nearly all of the native NVs we probed have a high fluorescence contrast in the ODMR spectrum and long T1 times typical of those found in much larger (>100 nm) nanodiamonds.

5 Future entangled quantum sensors in nanodiamonds

Looking toward the future, we note that there have been a number of suggestions that the quantum properties of single-color centers in small nanodiamonds will give improved bio-sensing capabilities. Thus far however, few of the quantum properties of

the NV have been used for sensing, even in bulk diamond. Therefore, it is important to ask what quantum effects we should strive for in our small nanodiamonds. To this end, we propose the development of nanodiamonds with two or more coupled NVs acting as a crude quantum computer. NVs are so far unique in their ability to satisfy all requirements of a quantum computer at room temperature (Neumann et al., 2010; Maurer et al., 2012). However, in the past, even in bulk diamonds, the problem of creating pairs of coupled NVs has been a difficult and highly improbable task. Fortunately, as mentioned above, near-deterministic NV pairs can now be created with shallow implantation in bulk diamond provided it is first activated with sulfur (Lühmann et al., 2021). These same implantation techniques can in principle be applied to nanodiamond, the only question is how small can the nanodiamonds be.

Assuming that multiple NVs can eventually created in nanodiamonds small enough for biological applications, we next consider what quantum algorithm might be used. As an initial goal we suggest fabrication of a magnetic gradiometer consisting of a

singlet state produced by quantum gates applied to two or more coupled NVs in a small nanodiamond. Such a two-qubit sensor could selectively observe nearby electron and nuclear spins, due to their relatively large gradients, while simultaneously suppressing the strong background magnetic fields that are present in the environment. If implemented with coherent subtraction as could be achieved with quantum logic, this gradiometer could also suppress quantum noise leading to even greater sensitivity.

6 Conclusion and outlooks

In this perspective, we discussed recent experiments that attempt to overcome the fabrication and performance limitations of small FNDs. To validate some of these experiments, we reproduced and optimized them, and in the best cases were able to create diamond color centers like the NV or SiV which provide more convincing evidence of diamond growth than in the original papers. In addition, we even used the NV as a built-in sensor to evaluate the quality of the grown nanodiamonds.

Future work includes optimizing the molecule-seeded growth technique to produce a higher yield of FNDs. In addition, for biosensing applications we plan to grow an upconversion phosphor shell, like Er:YLF, on these diamonds. If successful, infrared excitation of the shell would produce the green light needed to excite the NVs with minimal background biofluorescence fluorescence thus making the diamonds more visible in biological tissue samples.

Further into the future we plan to grow nanodiamonds precisely coupled NV centers with the aim of making them into quantum-enhanced sensors. This will also include adding isotopes like carbon 13 or nitrogen 15 to the seed molecule to produce NV quantum registers with long-term quantum memories. Finally, we note that these innovative nanodiamond growth techniques hold promise for virtually any industrial application of nanodiamonds that can benefit from highly scalable, low-cost growth.

References

Alkahtani, M., and Hemmer, P. (2020). Charge stability of nitrogen-vacancy color centers in organic nanodiamonds. *Opt. Mater. Express* 10 (5), 1224–1231. doi:10.1364/OME.392503

Alkahtani, M. H., Alghannam, F., Jiang, L., Almethen, A., Rampersaud, A. A., Brick, R., et al. 2018. "Fluorescent nanodiamonds: Past, present, and future." *Nanophotonics* 7 (8):1423–1453. doi:10.1515/nanoph-2018-0025

Alkahtani, M., Lang, J., Naydenov, B., Jelezko, F., and Hemmer, P. (2019). Growth of high-purity low-strain fluorescent nanodiamonds. *ACS Photonics* 6 (5), 1266–1271. doi:10.1021/acsphotonics.9b00224

Alkahtani, M., Alzahrani, Y., Janssen, J., Meijer, J., and Hemmer, P. 2023. "Co-localization of SiV and NV center in nanodiamonds." *In preparation*.

Badzigg, P., Verwoerd, W. S., Ellis, W. P., and Greiner, N. R. (1990). Nanometre-sized diamonds are more stable than graphite. *Nature* 343 (6255), 244–245. doi:10.1038/343244a0

Boudou, J.-P., Julia, T., Reuter, R., Thorel, A., Curmi, P. A., Jelezko, F., et al. (2013). Fluorescent nanodiamonds derived from HPHT with a size of less than 10nm. *Diam. Relat. Mater.* 37, 80–86. doi:10.1016/j.diamond.2013.05.006

Chang, S. L. Y., Reineck, P., Krueger, A., and Mochalin, V. N. (2022). Ultrasmall nanodiamonds: Perspectives and questions. *ACS Nano* 16 (6), 8513–8524. doi:10.1021/acs.nano.2c00197

Dahl, J. E., Liu, S. G., and Carlson, R. M. K. (2003). Isolation and structure of higher diamondoids, nanometer-sized diamond molecules. *Science* 299 (5603), 96–99. doi:10.1126/science.1078239

Dahl, J. E. P., Michael Moldowan, J., Wei, Z., Lipton, P. A., Peter, D., Gat, R., et al. (2010). Synthesis of higher diamondoids and implications for their formation in petroleum. *Angew. Chem. Int. Ed.* 49 (51), 9881–9885. doi:10.1002/anie.201004276

Davydov, V. A., Rakhamanina, A. V., Lyapin, S. G., Ilichev, I. D., Boldyrev, K. N., Shiryaev, A. A., et al. (2014). Production of nano- and microdiamonds with Si-V and N-V luminescent centers at high pressures in systems based on mixtures of hydrocarbon and fluorocarbon compounds. *Jetp Lett.* 99 (10), 585–589. doi:10.1134/s002136401410004x

Dovzhenko, Y., Casola, F., Schlotter, S., Zhou, T. X., Büttner, F., Walsworth, R. L., et al. 2016. "Imaging the spin texture of a skyrmion under ambient conditions using an atomic-sized sensor." *arXiv preprint arXiv:1611.00673*.

Flatae, A. M., Lagomarsino, S., Sledz, F., Soltani, N., Nicley, S. S., Haenen, K., et al. (2020). Silicon-vacancy color centers in phosphorus-doped diamond. *Diam. Relat. Mater.* 105, 107797. doi:10.1016/j.diamond.2020.107797

Funatsu, T., Taniyama, T., Tajima, T., Tadakuma, H., and Namiki, H. (2002). Rapid and sensitive detection method of a bacterium by using a GFP reporter phage. *Microbiol. Immunol.* 46 (6), 365–369. doi:10.1111/j.1348-0421.2002.tb02708.x

Greiner, N. R., Phillips, D. S., Johnson, J. D., and Volk, F. (1988). Diamonds in detonation soot. *Nature* 333 (6172), 440–442. doi:10.1038/333440a0

Hemmer, P., and Gomes, C. (2015). Single proteins under a diamond spotlight. *Science* 347 (6226), 1072–1073. doi:10.1126/science.aaa7440

Kamali, A. R., and Fray, D. J. (2015). Preparation of nanodiamonds from carbon nanoparticles at atmospheric pressure. *Chem. Commun.* 51 (26), 5594–5597. doi:10.1039/C5CC00233H

Data availability statement

The original contributions presented in the study are included in the article/supplementary material, further inquiries can be directed to the corresponding authors.

Author contributions

All authors listed have made a substantial, direct, and intellectual contribution to the work and approved it for publication.

Acknowledgments

We acknowledge the support of King Abdelaziz City for Science and Technology (KACST), Saudi Arabia. PH acknowledges the support of NSF grant 2032567.

Conflict of interest

The authors declare that the research was conducted in the absence of any commercial or financial relationships that could be construed as a potential conflict of interest.

Publisher's note

All claims expressed in this article are solely those of the authors and do not necessarily represent those of their affiliated organizations, or those of the publisher, the editors and the reviewers. Any product that may be evaluated in this article, or claim that may be made by its manufacturer, is not guaranteed or endorsed by the publisher.

Karim, A., Lyskov, I., Russo, S. P., and Alberto, P. (2020). An *ab initio* effective solid-state photoluminescence by frequency constraint of cluster calculation. *J. Appl. Phys.* 128 (23), 233102. doi:10.1063/5.0033417

Kaviani, M., Peter, D., Aradi, B., Frauenheim, T., Chou, J.-P., and Adam, G. (2014). Proper surface termination for luminescent near-surface NV centers in diamond. *Nano Lett.* 14 (8), 4772–4777. doi:10.1021/nl501927y

Kumar, A., Lin, P. A., Xue, A., Hao, B., and Mohan Sankaran, R. (2013a). Formation of nanodiamonds at near-ambient conditions via microplasma dissociation of ethanol vapour. *Nat. Commun.* 4 (1), 2618. doi:10.1038/ncomms3618 <https://www.nature.com/articles/ncomms3618#supplementary-information>

Kumar, A., Pin, A. L., Albert, X., Boyi, H., Yoke, K. Y., and Mohan Sankaran, R. (2013b). Formation of nanodiamonds at near-ambient conditions via microplasma dissociation of ethanol vapour. *Nat. Commun.* 4, 2618. Available at: doi:10.1038/ncomms3618 <https://www.nature.com/articles/ncomms3618#supplementary-information>

Lewis, R. S., Tang Ming, J. F. W.E. A., Steel, E., and Steel, E. (1987). Interstellar diamonds in meteorites. *Nature* 326 (6109), 160–162. doi:10.1038/326160a0

Liu, W., Alam, Md N. A., Liu, Y., Agafonov, V. N., Qi, H., Koynov, K., et al. (2022). Silicon-vacancy nanodiamonds as high performance near-infrared emitters for live-cell dual-color imaging and thermometry. *Nano Lett.* 22 (7), 2881–2888. doi:10.1021/acs.nanolett.2c00040

Lühmann, T., Meijer, J., and Pezzagna, S. . (2021). Charge-assisted engineering of color centers in diamond. *Phys. status solidi (a)* 218 (5), 2000614. doi:10.1002/pssa.202000614

Maurer, P. C., Kucsko, G., Latta, C., Jiang, L., Yao, N. Y., Bennett, S. D., et al. 2012. "Room-temperature quantum bit memory exceeding one second." *Science* 336 (6086): 1283–1286. doi:10.1126/science.1220513

Miller, B. S., Bezing, L., Harriet, D., Gliddon, Da H., Gavin, D., Dobson, P. J., et al. (2020). Spin-enhanced nanodiamond biosensing for ultrasensitive diagnostics. *Nature* 587 (7835), 588–593. doi:10.1038/s41586-020-2917-1

Neumann, P., Kolesov, R., Naydenov, B., Beck, J., Rempp, F., Steiner, M., et al. (2010). Quantum register based on coupled electron spins in a room-temperature solid. *Nat. Phys.* 6 (4), 249–253. doi:10.1038/nphys1536

Park, S., Abate, I. I., Liu, J., Wang, C., Jeremy, E. P., Carlson, R. M. K., et al. 2020. "Facile diamond synthesis from lower diamondoids." *Sci. Adv.* 6 (8):eaay9405. doi:10.1126/sciadv.aay9405

Peng, J. L., Orwa, J. O., Jiang, B., Prawer, S., and Bursill, L. A. (2001). Nano-Crystals Of C-Diamond, N-Diamond And I-Carbon Grown In Carbon-Ion

Implanted Fused Quartz. *Int. J. Mod. Phys. B* 15 (23), 3107–3123. doi:10.1142/s0217979201007208

Perevedentseva, E., Lin, Yu-C., and Cheng, C.-L. (2021). A review of recent advances in nanodiamond-mediated drug delivery in cancer. *Expert Opin. Drug Deliv.* 18 (3), 369–382. doi:10.1080/17425247.2021.1832988

Pezzagna, S. ., and Meijer, J. (2021). Quantum computer based on color centers in diamond. *Appl. Phys. Rev.* 8 (1), 011308. doi:10.1063/5.0007444

Qureshi, S. A., Hussain, L., Aman, H., Trong-Nghia, Le, and Rafique, M. (2022). Recent development of fluorescent nanodiamonds for optical biosensing and disease diagnosis. *Biosensors* 12 (12), 1181. doi:10.3390/bios12121181

Shen, Y., Su, S., Wen, Z., Cheng, S., Xu, T., Yin, K., et al. (2021). Sub-4 nm nanodiamonds from graphene-oxide and nitrated polycyclic aromatic hydrocarbons at 423 K. *ACS Nano* 15 (11), 17392–17400. doi:10.1021/acsnano.1c00209

Stein, S. E. (1990). Diamond and graphite precursors. *Nature* 346 (6284), 517. doi:10.1038/346517a0

Su, Z., Zhou, W., and Zhang, Y. (2011b). New insight into the soot nanoparticles in a candle flame. *Chem. Commun.* 47 (16), 4700–4702. doi:10.1039/C0CC05785A

Su, Z., Zhou, W., and Zhang, Y. (2011a). New insight into the soot nanoparticles in a candle flame. *Chem. Commun. (Camb)* 47 (16), 4700–4702. doi:10.1039/c0cc05785a

Tzeng, Y.-K., Zhang, J. L., Lu, H., Ishiwata, H., Dahl, J., RobertCarlson, M. K., et al. (2017). Vertical-substrate MPCVD epitaxial nanodiamond growth. *Nano Lett.* 17 (3), 1489–1495. doi:10.1021/acs.nanolett.6b04543

Visscher, G. T., Nesting, D. C., Badding, J. V., and Bianconi, P. A. (1993). Poly(phenylcarbyne): A polymer precursor to diamond-like carbon. *Science* 260 (5113), 1496–1499. doi:10.1126/science.260.5113.1496

Vlasov, I. I., Shiryaev, A. A., Rendler, T., Steinert, S., Lee, S.-Y., Antonov, D., et al. (2014). Molecular-sized fluorescent nanodiamonds. *Nat. Nanotechnol.* 9 (1), 54–58. doi:10.1038/nnano.2013.255

Waddington, D. E. J., Boele, T., Rej, E., Reilly, D. J., et al. (2019). Phase-encoded hyperpolarized nanodiamond for magnetic resonance imaging. *Sci. Rep.* 9 (1), 5950. doi:10.1038/s41598-019-42373-w

Zapata, T., Bennett, N., Struzhkin, V., Fei, Y., Jelezko, F., Biskupek, J., et al. 2017. "Organic nanodiamonds." *arXiv preprint arXiv:1702.06854*.